Article (refereed) - postprint

Fleischer, Katrin; Rammig, Anja; De Kauwe, Martin G.; Walker, Anthony P.; Domingues, Tomas F.; Fuchslueger, Lucia; Garcia, Sabrina; Goll, Daniel S.; Grandis, Adriana; Jiang, Mingkai; Haverd, Vanessa; Hofhansl, Florian; Holm, Jennifer A.; Kruijt, Bart; Leung, Felix; Medlyn, Belinda E.; Mercado, Lina M.; Norby, Richard J.; Pak, Bernard; von Randow, Celso; Quesada, Carlos A.; Schaap, Karst J.; Valverde-Barrantes, Oscar J.; Wang, Ying-Ping; Yang, Xiaojuan; Zaehle, Sönke; Zhu, Qing; Lapola, David M.. 2019. **Amazon forest response to CO2 fertilization dependent on plant phosphorus acquisition.** *Nature Geoscience*, 12 (9). 736-741.
https://doi.org/10.1038/s41561-019-0404-9

**$CO_2$ fertilization of the Amazon forest hinges on plant phosphorus use and acquisition**

We present here supplementary information to the main text of the study "$CO_2$ fertilization of the Amazon forest hinges on plant phosphorus use and acquisition" by Fleischer et al., submitted to Nature Geoscience.

The individual models' biomass C responses to $eCO_2$ are shown in **Extended Data Figure 1**, where the absolute and relative effect of $eCO_2$ on cumulative biomass C is included. The variation in their predictions among and within the model groups becomes apparent. While CNP models (in green) generally predict lower biomass C gain with $eCO_2$ compared to C-only (grey) and CN models (blue), some CNP models exceed predictions by the other model groups. Assumptions on how plant P use and P acquisition is dealt with in the models cause these diverging responses.

The individual models' performance in representing ambient conditions of key ecosystem variables are shown in **Extended Data Figure 2**. Models generally represented ambient conditions (GPP, NPP and LAI) well at the study site. GPP was lower than observed in all but two models, while the uncertainty around observed GPP is considerable (from 3.0-3.5 kg C $m^{-2}$ $yr^{-1}$)(see Extended Data Table 2). Given this observational uncertainty, we judge only ELM-FATES' ambient GPP as underestimated with certainty. For LAI, models either over- or underestimated LAI by about 1 $m^2$ $m^{-2}$, while ELM-ECA and ED2 produced too low ambient LAI around 4 $m^2$ $m^{-2}$. For biomass C, models diverged noticeably from 10 to more than 30 kg C $m^{-2}$. Biomass C is controlled by productivity and turnover dynamics simultaneously. Belowground components remain more uncertain and were not considered in the observational-based estimate here. Ambient annual biomass C increment varied strongly across the models, ranging from 5 to 114 g C $m^{-2}$ $yr^{-1}$, for which we included the Amazon-wide estimate of 64 g C $m^{-2}$ $yr^{-1}$ from Brienen et al. 2015 as an observation. Many models (CABLE-POP, CABLE-POP(CN), InLand) estimate ambient biomass C increment within the confidence interval of this estimate (45-78 g C $m^{-2}$ $yr^{-1}$). The actual observational estimate from our site is 23 g C $m^{-2}$ $yr^{-1}$, so that other models are in better agreement with this lower estimate (CABLE, GDAY, LPJ-GUESS, GDAY(CN), JULES). The site estimate is associated to higher uncertainties due to few censuses. These findings underlines the need for more long term growth measurements. For both, biomass C and biomass C increment, there was no clear pattern between the model groups, so that these differences did not affect the conclusions of our study.

The models simulated less than 1.1 g labile P $m^{-2}$ to 4 m depth in the ambient run (with the exception of ELM-CTC), which is the plant available soil P. Observations indicate 1.6 g resin P $m^{-2}$ to 30 cm depth. Resin P is considered to be directly plant-available, representing the modelled soil labile P pool, although direct comparisons are hampered as P fractionations are operationally defined. Observations are thus slightly higher but both modelled and observed values on soil labile P are considered to be very low and the resulting modelled P limitation to be realistic.

The individuals models' simulation results on the relative $eCO_2$ effect on primary productivity (GPP, NPP), plant tissue C stocks and plant CUE are shown in **Extended Data Figure 3**. The models' plant C allocation fractions and the respective relative effect of $eCO_2$ thereon is shown in **Extended Data Figure 4**. The individuals models' simulation results on the relative $eCO_2$ effect on N and P uptake, NUE and PUE, as well as plant tissue stoichiometry is shown in **Extended Data Figure 5**.

The relationship between $eCO_2$ induced P uptake, fine root allocation, and the respective return of P uptake per unit fine root allocation for three CNP models are shown in **Extended Data Figure 6**. The three models (ELM-ECA, GDAY, and ORCHIDEE) simulated a higher fine root investment with $eCO_2$, but a heightened relative return of P was only achieved temporarily, after some time, or not at all. The absolute effect of $eCO_2$ on NUE, PUE and stoichiometry for the individual models is shown in **Extended Data Figure 7**. Both CN and CNP versions of GDAY and CABLE-POP were included in the model ensemble, allowing the N and P effect alone to be inferred. Their respective CN versions, and some other CN models, indicated that N limitation occurred, as leaf and biomass C:N were predicted to increase under eCO2 (Extended Data Fig. 7). The inclusion of both CN and CNP versions for GDAY and CABLE-POP supported the fact that P cycle limitations reduced the $eCO_2$ induced biomass C sink, as the main comparison across the C, CN and CNP model group indicated.

Model driving data of precipitation are plotted as annual precipitation over the course of the 15 year study period in **Extended Data Figure 8**. Precipitation (and other climate) data was derived from the K34 fluxtower, which experienced two years of strong precipitation deficit during the study period, 2000 and 2009. The relative $eCO_2$ response of GPP and NPP is plotted against annual precipitation in the **Extended Data Figure 9** to test for potential interactions of $eCO_2$ and droughts in the study region. While some

models show a significant effect of precipitation on the strength of the $eCO_2$ effect on GPP, the slope of the line is very shallow, so that we can conclude that variations in water availability contributed little to the simulated $eCO_2$ effect in our study.

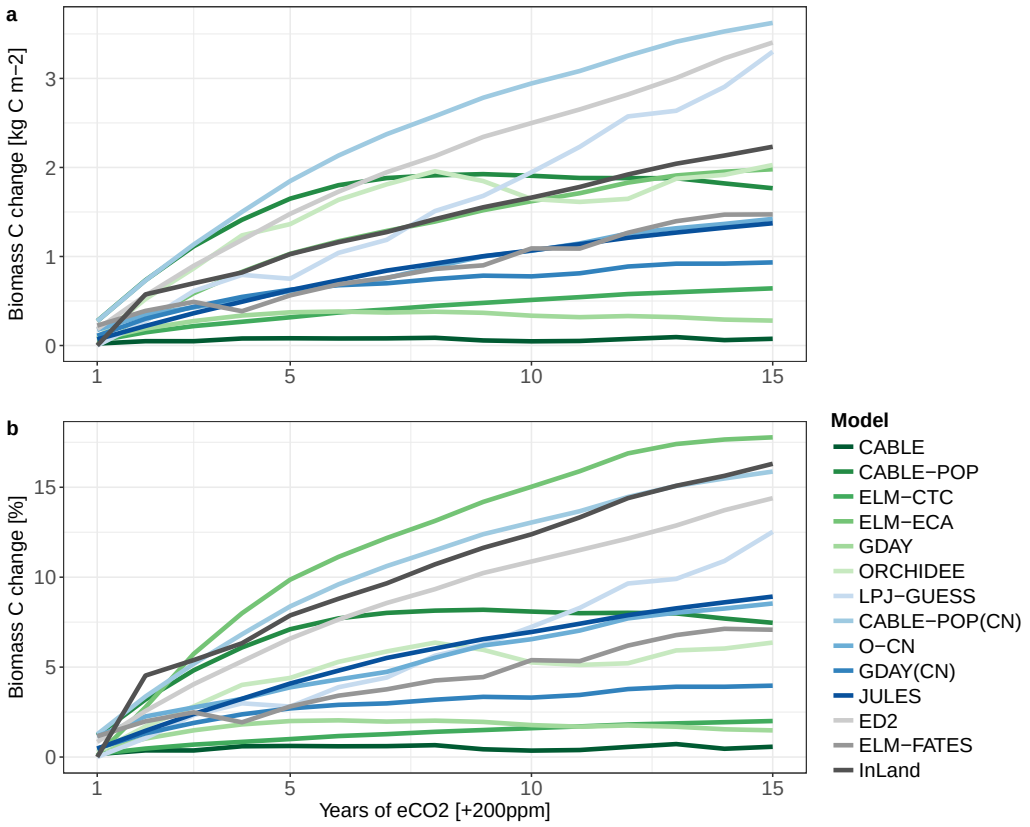


**Extended Data Figure** 1: **Cumulative effect of $eCO_2$ on biomass C per model. a**, Absolute cumulative effect on biomass C in kg C $m^{-2}$, and **b**, relative cumulative effect on biomass C in %. See legend for individual model names. C-only models are in shades of grey, CN models are depicted in shades of blue and CNP models are depicted in shades of green.

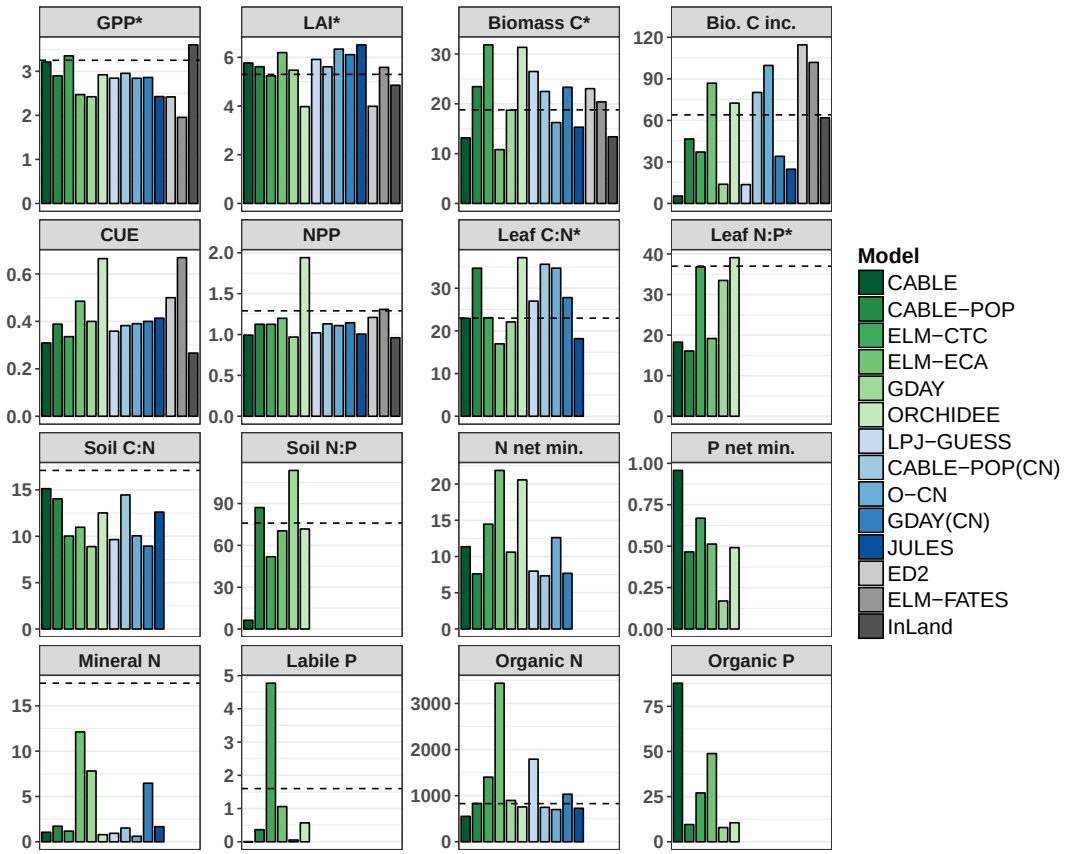


**Extended Data Figure** 2: **Ambient model conditions compared to *in situ* observations.** Individual models' values are mean conditions over the ambient simulation. Horizontal dotted lines indicate observations when available (see sources in Extended Data Table 1). Measurements marked with a $\star$ were provided to modelers beforehand. C fluxes (GPP, NPP) are in kg C $m^{-2}$ $yr^{-1}$, biomass C is aboveground only in kg C $m^{-2}$, and biomass C increment in g C $m^{-2}$ $yr^{-1}$. The observational estimate for biomass C increment is based on the Amazon-wide estimate from Brienen et al. 2015 (64 g C $m^{-2}$ $yr^{-1}$ for the 2000s, C.I. 45-78 g C $m^{-2}$ $yr^{-1}$). CUE is calculated as the ratio of NPP per GPP. LAI is in $m^2/m^2$. Leaf and soil stoichiometry are ratios of C, N and P content in dry matter, respectively. Leaf stoichiometry was parameterised only in some models (see Extended Data Table 2). Fluxes of net N and P mineralisation are in g N/P $m^{-2}$ $yr^{-1}$. Soil mineral N pool and labile P pool (both considered plant-available), as well as soil organic N and P pool, are in g N/P $m^{-2}$. Observations for soil nitrogen content are based on top 10 cm, and for labile P on top 30cm. Modeled values are based on a soil depth of 4m. See legend for individual model names. C-only models are in shades of grey, CN models are depicted in shades of blue and CNP models are depicted in shades of green.

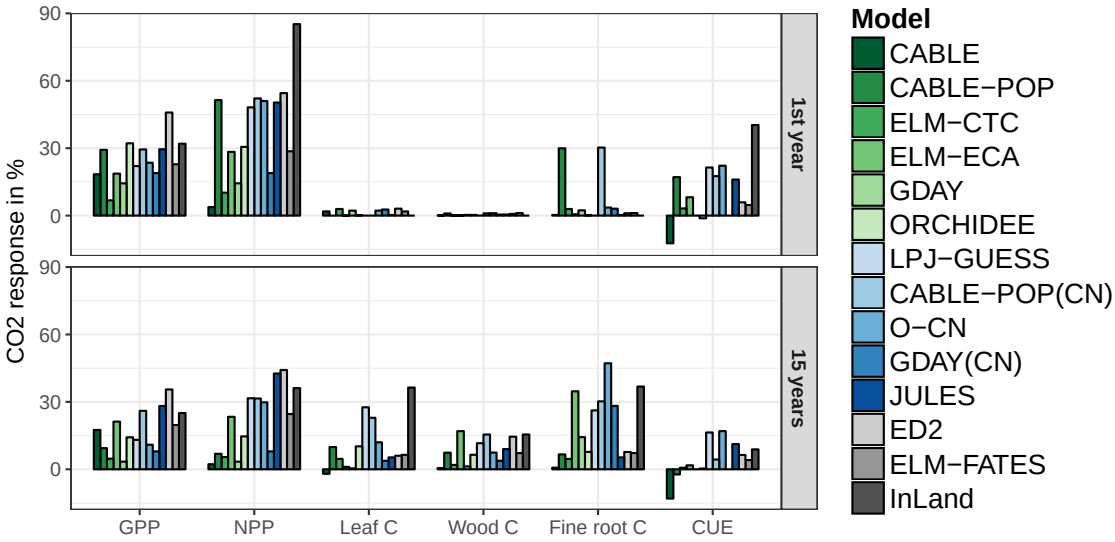


**Extended Data Figure** 3: **Relative effect of $eCO_2$ on GPP, NPP, leaf C, wood C, fine root C and plant CUE.** Shown are initial effects (1st year) on top and final effect after 15 years of $eCO_2$ (mean of 13th to 17th year), both in %. See legend for individual model names. C-only models are in shades of grey, CN models are depicted in shades of blue and CNP models are depicted in shades of green.


**Extended Data Figure** 4: **Ambient C allocation to plant tissues and the effect of $eCO_2$ thereon.** Mean and standard deviation of ambient C allocation to leaf, wood, coarse and fine root per model in % (top), and annual effect of $eCO_2$ on C allocation fractions over 15 years per model in % (bottom). See legend for tissue compartments; leaf is displayed in green, wood in red, coarse root in dark blue and fine root in light blue. Note individual y-axis scaling in bottom graph.

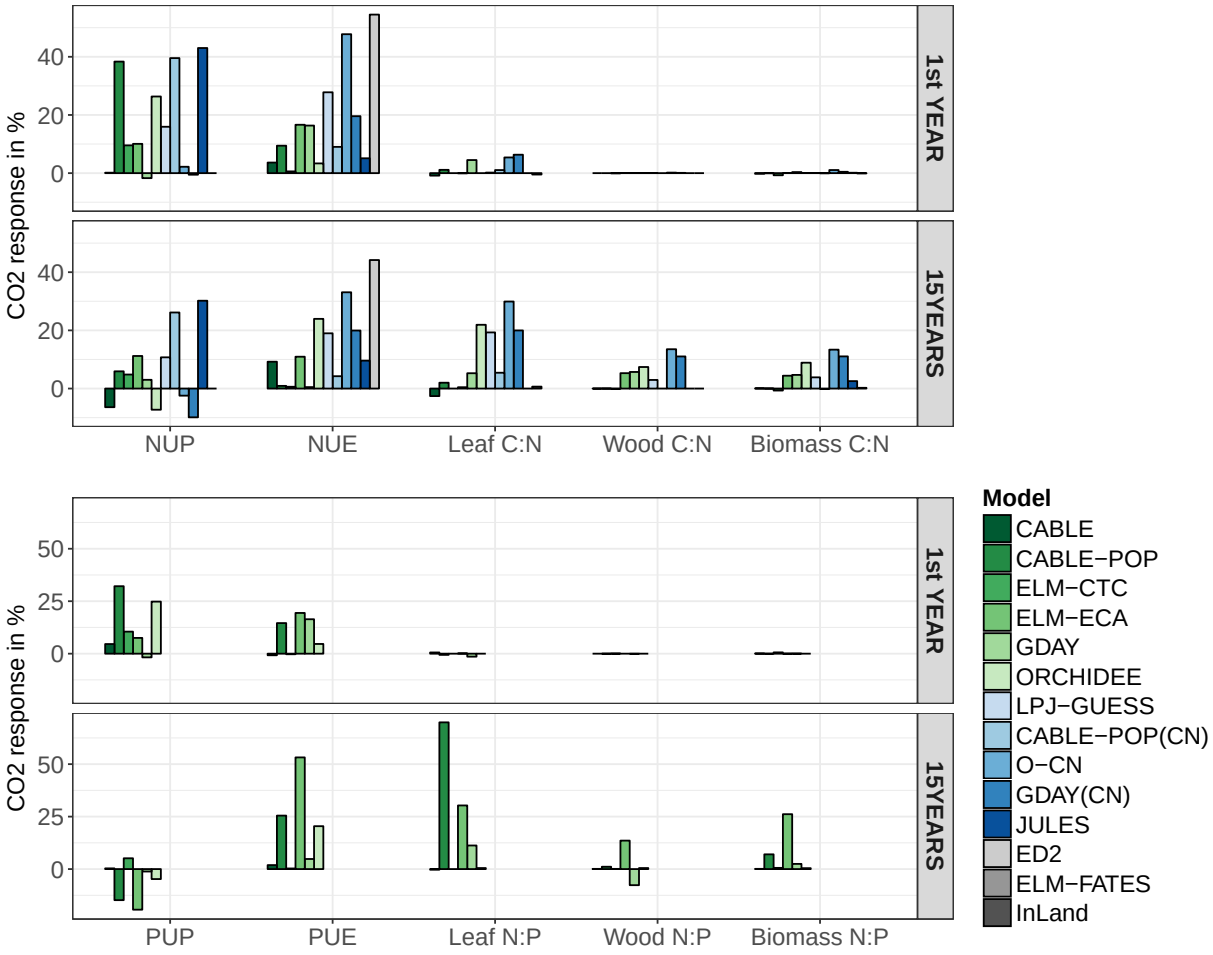


**Extended Data Figure** 5: **Relative effect of $eCO_2$ on N and P uptake, NUE and PUE, and biomass stoichiometry per model.** Shown are initial effects (1st year), and final effects after 15 years of fumigation (mean of 13th to 17th year), for N uptake (NUP), N use efficiency (NUE), leaf C:N, Wood C:N, and biomass C:N for all CN and CNP models, in % (top). Further displayed are P uptake (PUP), P use efficiency (PUE), leaf N:P, wood N:P, and biomass N:P for all CNP models, in % (bottom). See legend for individual model names. C-only models are in shades of grey, CN models are depicted in shades of blue and CNP models are depicted in shades of green.

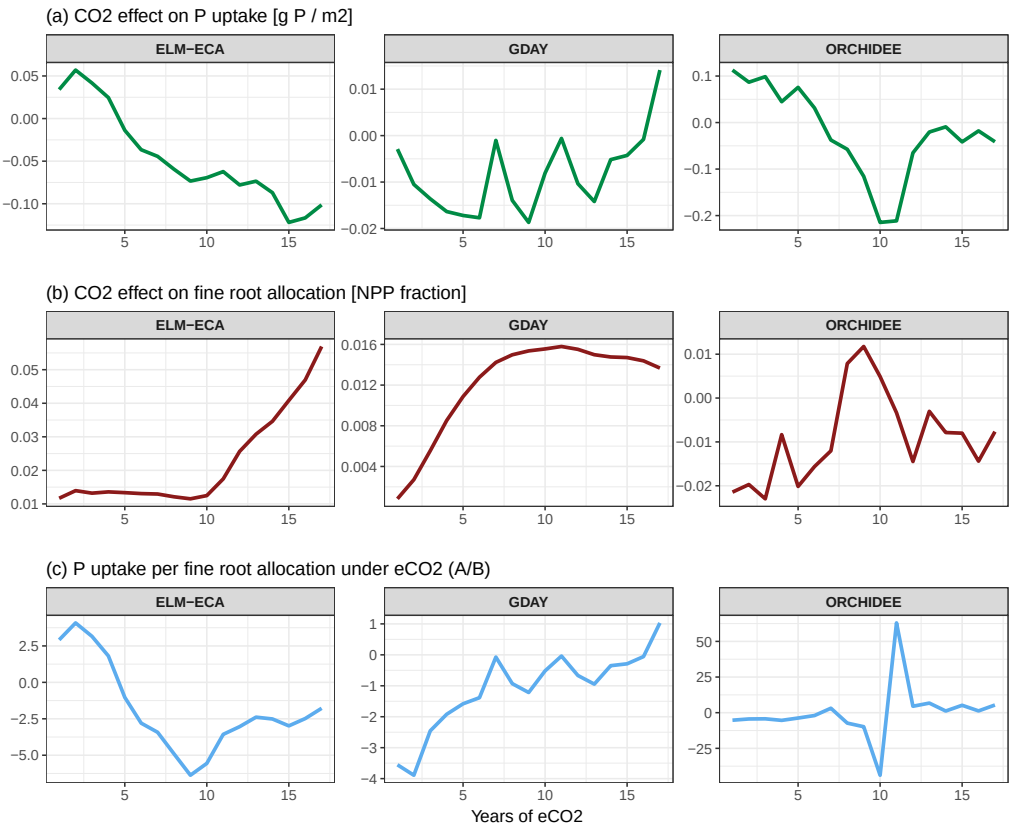


**Extended Data Figure** 6: **Effect of $CO_2$ on P uptake, fine root investment and the resulting P uptake per fine root investment. a**, $CO_2$ effect on P uptake, **b**, $CO_2$ effect on fine root allocation, and **c**, P uptake gain per fine root investment (a/b). Shown for the three CNP models that predict higher fine root investment with $eCO_2$, see plot title for individual model names.

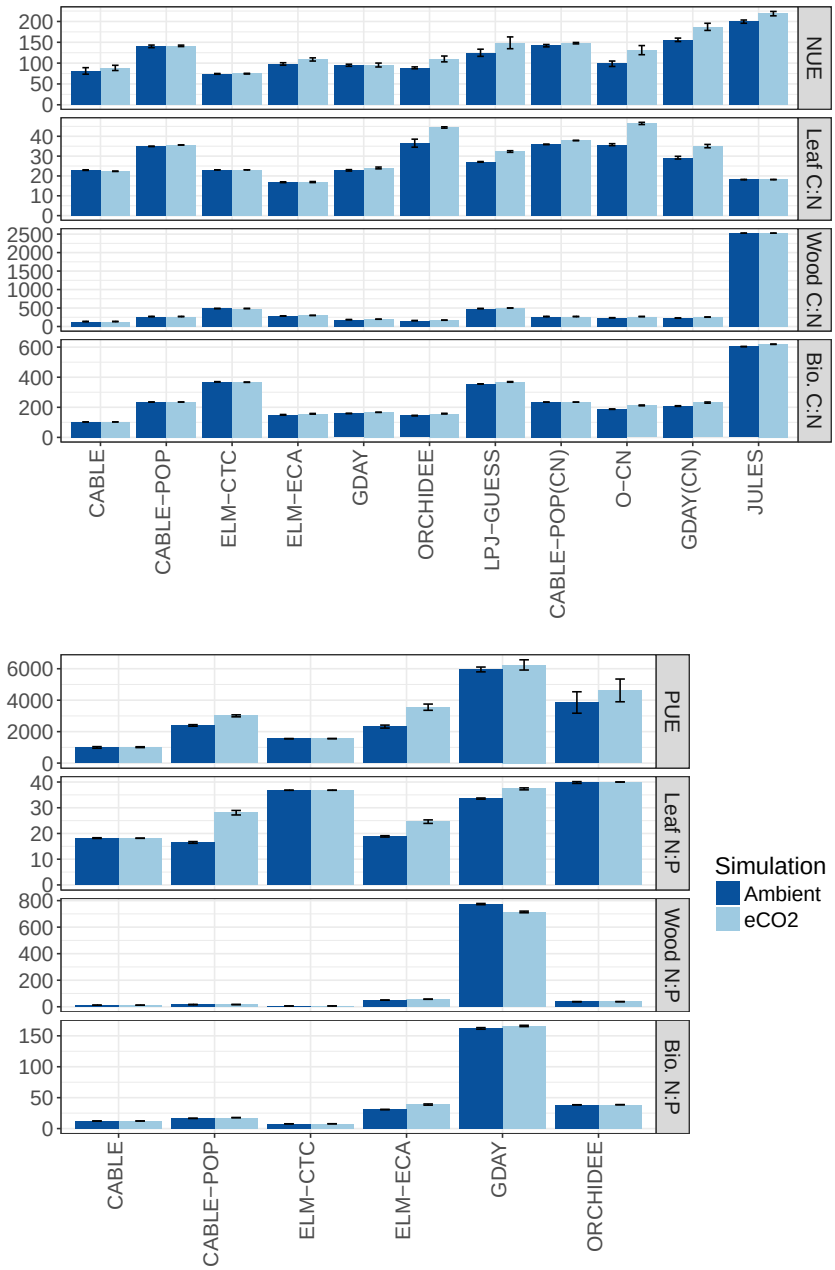


**Extended Data Figure 7: Absolut $CO_2$ effect on nutrient use efficiency and biomass stoichiometry per model.** Shown are the absolut difference between ambient and $eCO_2$ simulation run at the end of the 15 year simulation experiment (mean and standard deviation of 13th to 17th year) for nitrogen use efficiency (NUE), leaf C:N, wood C:N, and plant biomass C:N for CN and CNP models (top), and for phosphorus use efficiency (PUE), leaf N:P, wood N:P, and plant biomass N:P for CNP models (bottom). See x-axis for individual model names.

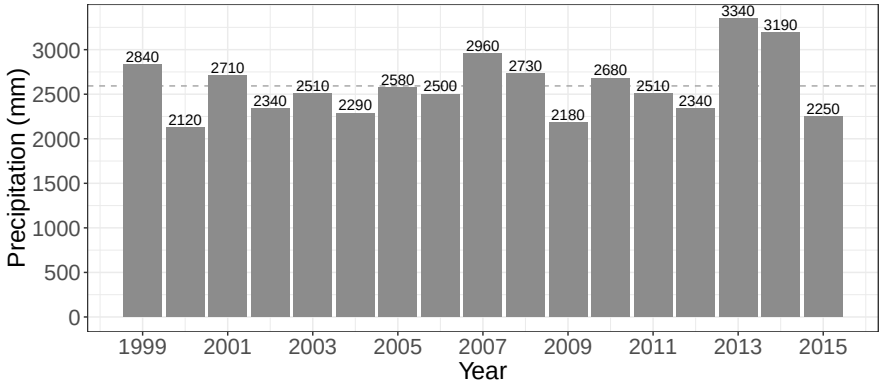


**Extended Data Figure** 8: **Annual precipitation from the fluxtower K34, used as model driving data.** Shown are sums of annual precipitation in mm, rounded to the nearest tenth. Note that years represent Southern hemisphere growing season, i.e. 01/07/year to 30/06/year+1. The mean annual precipation of 2590mm is underlain as a dotted line.

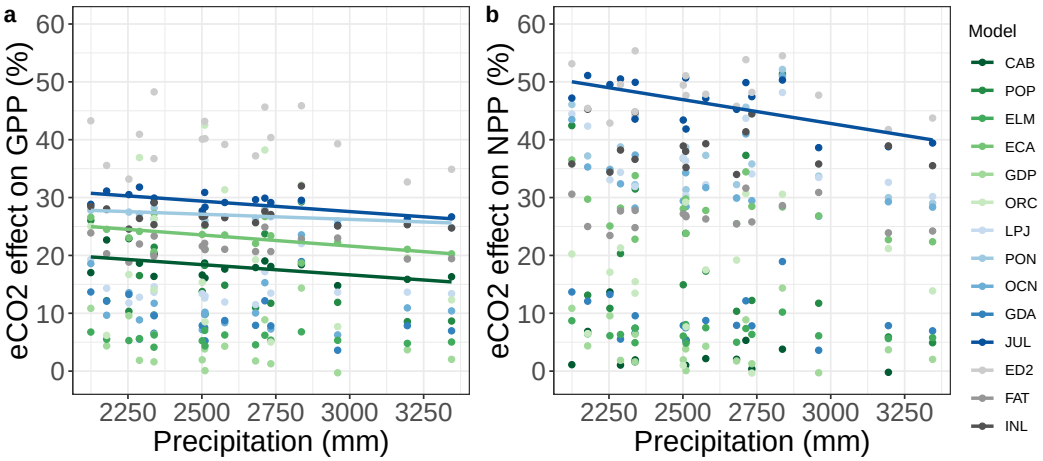


**Extended Data Figure** 9: **Effect of precipitation on the individual models' eCO$_2$ effect on GPP and NPP. a**, eCO$_2$ effect on gross primary production (GPP) (in %) and **b**, eCO$_2$ effect on net primary production (NPP), both against sum of precipitation (in mm) throughout the experimental phase (1999-2015). See legend for individual model names. C-only models are in shades of grey, CN models are depicted in shades of blue and CNP models are depicted in shades of green. Only significant ($p<0.05$) linear regression lines are drawn in the respective model colour.